Jurnal
Teknologi

Full Paper

The Influence of Ni-Ti Ratio on the Reversible Austenite-Martensite Transformation and mechanical properties Produced by Metal Injection Moulding

Article history
Received
15 January 2015
Received in revised form
30 April 2015
Accepted
31 May 2015

Rosliza Razali[a], Zulaila Abdullah[a], Istikamah Subuki[a],
Norhamidi Muhamad[b], Muhammad Hussain Ismail[c]*

[a]Faculty of Chemical Engineering, Universiti Teknologi MARA, 40450 Shah Alam Selangor, Malaysia
[b]Faculty of Engineering & Built Environment, Universiti Kebangsaan Malaysia, 43600, Bangi Selangor, Malaysia
[c]Centre for Advanced Materials Research (CAMAR), Faculty of Mechanical Engineering, MARA, 40450 Shah Alam Selangor, Malaysia

*Corresponding author
hussain305@salam.uitm.edu.my

Graphical abstract

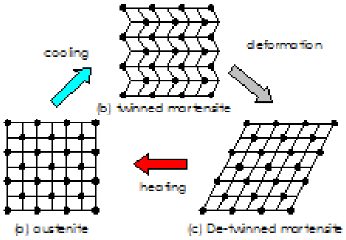

Abstract

This paper highlights the influence of Ni-Ti ratio on the phase constituents, the reversible austenite-martensite transformation and mechanical properties produced by metal injection molding (MIM). The binder system used was mainly palm stearin with minor fraction of polyethylene. Injection moulding was done successfully at 130˚C to form tensile shape samples. It was followed by solvent extraction, thermal debinding at 500°C and subsequently sintered in high vacuum at 1100˚C. The result showed that as the Ni content increased, the fraction of austenite phase also increased owing to greater fraction of transient liquid phase formation during the sintering, thus improved the mechanical tensile properties. However, the reversible austenite to martensite phase transformation temperatures (PTTs) seemed to be broadened with increased Ni content due to formation of metastable R-phase.

Keywords: Metal injection moulding, austenite-martensite, elemental, NiTi alloy

1.0 INTRODUCTION

Nickel titanium (NiTi) or also known as Nitinol is an inter-metallic compound of nickel and titanium [1], generally presents in nearly-equiatomic (50 at%Ni – 50 at%Ti) [2]. The alloy is known to exhibit two unique properties, namely shape memory effect (SME) and pseudoelasticity (PE) [3]. SME is the ability of the material to be deformed at low temperature and then revert to its original shape upon heating above a critical temperature (austenite finish temperature, A_f). PE is the ability of the material to return to its original shape upon unloading after large deformation, principally similar to mechanism of stretching a rubber band [4].

It is well known that there are basically two crystallographic phases in NiTi which may be experienced through phase change, namely austenite and martensite [5], depending on the temperature and deformation mechanism experienced. The austenite is generally referred to as the parent (B2) phase, as shown schematically in Fig. 1(a), and is known as a phase which is very stable and strong at high temperature and which has a single variant with body-centred cubic (BCC) crystal structure [6]. On the other hand,

76:10 (2015) 75–83 | www.jurnalteknologi.utm.my | eISSN 2180–3722 |

martensite, or the B19' phase, which is relatively soft and stable at low temperature, can be easily deformed either by temperature (the so-called twinned martensite) [Fig. 1 (b)] or stress (de-twinned martensite) [Fig. 2 (c)].

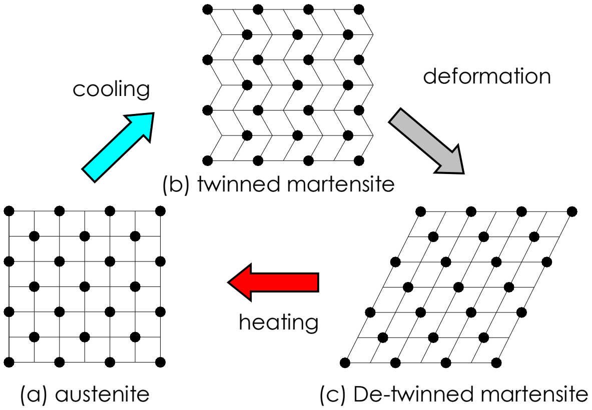

Figure 1 Three possible crystallographic orientations in NiTi.

Owing to the extraordinary properties of SME and PE, a number of investigations and reviews related to biomedical applications have been presented [6-7] Among them are orthodontic wires, orthopaedic implants for osteosynthesis, guide wires, stents for various applications, components in minimal invasive surgical devices and bone substitution materials [5-7].

In order for the NiTi to exhibit excellent SME and PE to suit certain applications, some of the important aspects has to be taken into consideration. One of the critical issues is to attain microstructural homogeneity of Ni and Ti composition, particularly for processing route starting with elemental Ni and Ti powders. This is due to the fact that other secondary phases, namely Ni_3Ti and $NiTi_2$ are always co-exist with NiTi during processing. These secondary phases are known as brittle in nature and do not exhibit both properties SME and PE , thus limiting the capability of the alloy [6]. The second aspect is the capability of alloy to demonstrate reversible phase transformation from the austenitic (B2) to martensitic phase (B19'), which is generally characterized by a differential scanning calorimetry (DSC). From the biomedical implant point of view, it is important for the processed NiTi to exhibit the austenite phase finish (A_f) at human body temperature (37°C) to ensure the implant can behave pseudoelastically, mimicking the properties of natural bone. This is due to the fact that greater sensitivity of the alloy to a minor variation of Ni and Ti composition. Many works have reported that when Ni content is greater than 50 at.%, an increase of 0.1 at.% Ni could result in a 10°C decrease in martensite phase start temperature, M_s [8,9]. Therefore, variations in the composition of Ni or Ti would alter the transformations temperature [8]. Besides that, PTTs are also influenced by the existing phases in the as-sintered sample. The fraction of secondary phases such as $NiTi_2$ and Ni_3Ti and the impurity levels, particularly oxygen and carbon significantly broaden the reversible PTTs.

In the present work, NiTi alloys with different Ni-Ti ratio have been produced by an advanced powder metallurgy (PM) process, namely metal injection moulding (MIM) starting with elemental powders of Ni and Ti. The composite binder system of palm stearin (PS) and polyethylene (PE) was used to facilitate mixing and moulding. This study emphazized on the level of microstructural homogeneity by XRD followed by back-scattered scanning electron microscopy (SEM) analysis. The influence of NiTi ratio on reversible phase transformation temperatures (PTTs) was further anlaysed by DSC. The mechanical properties by tensile test was also conducted to investigate the effect of Ni ratio in the alloy.

2.0 EXPERIMENTAL

2.1 Raw Materials and Feedstock Preparation

The elemental powders used in the present work were Ni and Ti with an average particle size of 8 and 11 μm, respectively. Both powder are spherical in shape as shown in Fig. 2 that is known can facilitate the feedstock flow during injection moulding process. Three atomic ratios (at%) of Ni to Ti were investigated; 50-50, 50.4-49.6 and 50.8-49.2 and the powder loading was kept constant 65.5vol% for all compositions. The elemental powders were blended using a stainless steel ball mill for 4 hours with a ball-to-powder ratio of 2:1 to ensure uniform powder distribution. The mixing process was carried out using Haake Rheomix Internal Mixer at temperature of 160˚C and 50 rpm [10]. The feedstock was then pelletized by keeping the blade rotating during cool down of mixing chamber.

2.2 Rheological Test and Injection Moulding Process

The feedstock flow was analyzed using a capillary rheometer, model RH2000 Bohlin at shear rate and barrel temperature ranging from 20 – 10,000 s^{-1} and 110 – 150°C, respectively. A tungsten carbide die with an orifice diameter and length of 1.0 mm and 16 mm, respectively, resulting in an aspect ratio (L/d) of 16 was used. The feedstock was subjected to a pre-test at a constant speed of 100 mm/min and a pressure of 2 MPa, to squeeze the air out of the sample before the shear viscosity at the first shear rate was measured. The viscosity data of the extruded feedstock against the increasing shear rate were recorded via the software. Injection moulding was carried out using a manually operated vertical injection moulding with a tensile shape cavity according to ASTM 638 type V as shown in Fig. 3 [11].

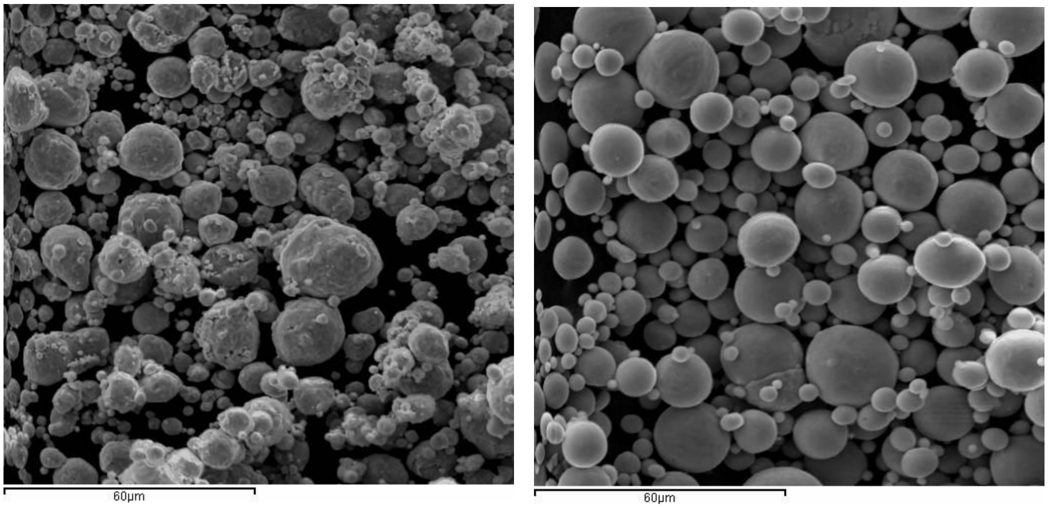

Figure 2 SEM of elemental powders ; (a) Ni and (b) Ti

2.3 Debinding and Sintering

The moulded samples were then immersed in a heptane solution at 60 ˚C for 5 hours to remove the primary binder of palm stearin. Thermal debinding and sintering processes were carried out using a vacuum furnace. Prior sintering at maximum temperature of 1100˚C, thermal debinding was done to eliminate the backbone binder of polyethylene (PE) at 500˚C. The summary of NiTi alloy processing is shown schematically in Fig. 3.

2.4 Characterization of Sintered Parts

Inter-metallic phase analysis of the as-sintered samples were initially characterized by a Rigaku X-Day Diffraction (XRD) with a diffraction angle 2θ within 30˚ and 90˚ at a scan speed of 1˚/min. The reversible austenite to martensite phase transformation temperatures (PTTs) was analysed by a Mattler Toledo Differential Scanning Calorimetry (DSC). The mechanical tensile test analysis was done at room temperature using an Instron machine at the speed rate of 0.5 mm/min. The fracture samples were examined by secondary SEM for clarification.

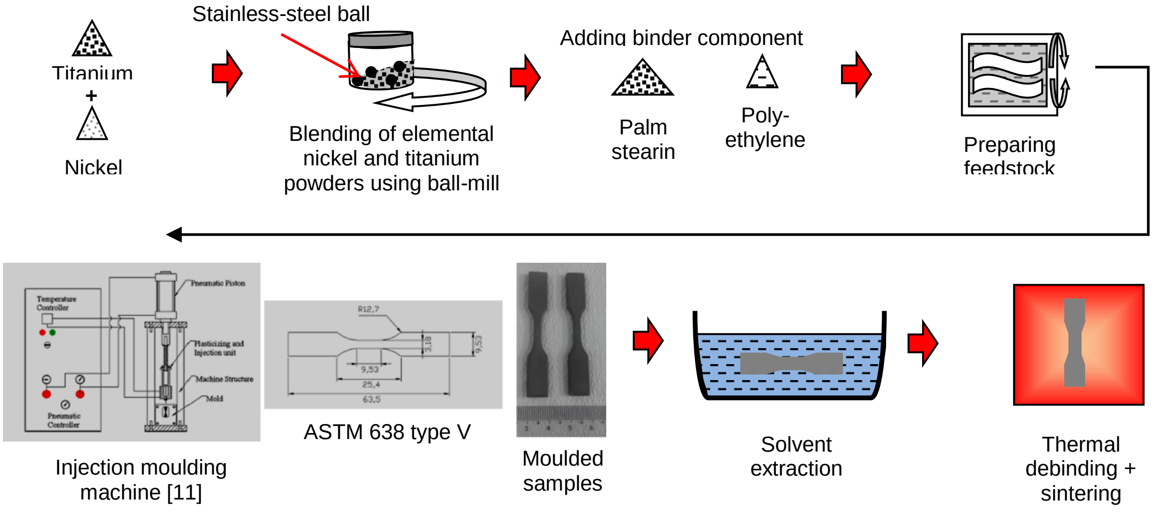

Figure 3 Schematic diagram of the MIM processing stages involved in the present work.

3.0 RESULTS AND DISCUSSION

3.1 Rheological Result & Moulding Analysis

Fig. 4 compares the rheological results; apparent viscosity versus shear rate for all compositions at different temperatures ranging from 110 and 150°C. It clearly shows that all feedstock compositions exhibit a similar pattern; viscosity decreasing with shear rate which corresponds to pseudoplastic behavior; the required flow properties in injection moulding process. It clearly shows that increasing the Ni content in the formulation resulted in slightly decrease in viscosity, particularly at the lower shear rate which was attributed from the finer powder size of Ni powder.

Increasing Ni content in the feedstock formulation would result in greater powder surface contact area to be coated with the binder and therefore, reducing the friction of the feedstock. As the shear rate was further increased, it was observed that the feedstocks exhibit a similar pattern of shear thinning with a nearly constant viscosity at the high shear rate (>2000 /s). The viscosity range obtained for all compositions in the present work was considerably low in comparison with the previous work conducted by Ismail [12], in which the viscosity at the lowest shear rate observed was in the range of 300 to 700 Pa.s, for the same powder loading employed (65.5vol%). Ismail used Ni and Ti powder size (D_{50}) of 15 µm and 32 µm, respectively, thus less surface area as compared to powder used in the present work.

During the injection molding process, it was observed that the green samples were successfully moulded at the barrel temperature of 130°C. Figure 3 shows the image of the defect free moulded samples. The total cycle time for each sample was approximately 5 minutes owing to manually operated process, taken into account the time to place the mould underneath the nozzle, injection moulding (~1-2 seconds), cooling stage, mould removal and removal of green samples from the mould. It was observed that the green samples produced had adequate strength to be handled after they were removed from the mould cavity.

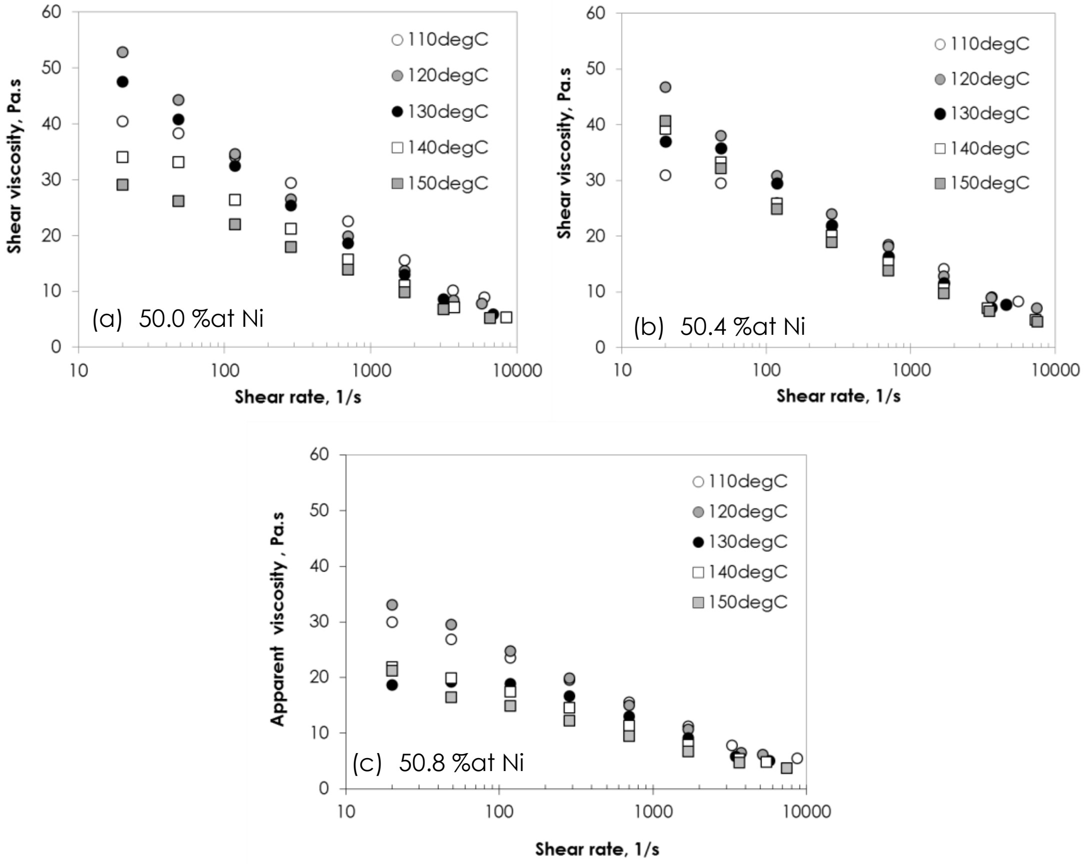

Figure 4 Rheological result of the Ni-Ti feedstock with different %at Ni.

3.2 XRD and SEM Analysis of As-Sintered Samples

Fig. 5 shows the XRD patterns of the sintered samples with different Ni-Ti ratios: (a) 50.0at%Ni, (b) 50.4at%Ni and (c) 50.8at%Ni. The result clearly shows that no significant difference of the corresponding peaks for Ni-rich samples (50.4at.%Ni and 50.8at.%Ni) in comparison with the 50.0at.%Ni. Generally, NiTi alloy can be categorized into two different types, austenitic (B2) or martensitic (B19'), depending on the thermo-mechanical treatment process carried out. The formation of NiTi phase, particularly B2 via complete inter-diffusion between elemental Ni and Ti is important during sintering as it will dictate the SME and PE performance during actual service condition. For instance in bone implant application, greater fraction of B2 phase is essential as it promotes excellent PE properties that mimicking the natural bone behaviour. Besides that, the formation of other secondary phases, particularly $NiTi_2$ and Ni_3Ti has to be minimized significantly as these phases are known as not exhibiting both SME and PE [9]. Furthermore, their corrosion resistance is also considerably low in comparison with the matrix of NiTi phase.

It was observed that the secondary phase of $NiTi_2$ was present in all sintered samples. However, their occurrence in the microstructure is believed to be very minimal. For the lowest Ni content (50at%Ni), besides $NiTi_2$, the Ni_3Ti phase was also present, thus, expecting lower mechanical strength of the corresponding alloy composition due to brittle nature of the phase. For the Ni-rich compositions (50.4 and 50.8at%Ni), greater fraction of NiTi (B2) phase was observed together with some fraction of B19' phase, indicating probably sufficient diffusion between elemental Ni and Ti powders during sintering in the present work. Furthermore, it was also expected that formation of transient liquid phase (TLP) during sintering that promoted better acceleration of the diffusion kinetics as discussed in previous work [12]. Owing to a greater diffusion rate of Ni compared to Ti, it was believed that the increase of the Ni content would result in better phase homogenezation; minimal fraction of secondary phases. The formation of secondary phases was unavoidable, particularly for Ti-rich composition (50at%Ni), a similar observation as demonstrated by Yen et al. [9]. Yen et al. [9] also claimed that the fraction of secondary phases reduced significantly as the Ni content increased.

Fig. 6 reveals the SEM micrograph of the as-polished sintered sample for 50.4at%Ni under back-scatted mode (BS). The result clearly shows different gray-scales, indicating different phases exist as a result of different energy absorbed. Study by E.Schüller (2005) [3] has stated that there are three different gray scales that represent different phases based on EDX analysis. The medium gray matrix phase corresponds well to NiTi, the needle-like structure which dissapears when heated represent the martensite phase and the dark gray phase which contributed from Ti content represent Ti-rich composition of $NiTi_2$. Besides that, study by Ismail (2012) [10] have stated that the needle-like structure is probably due to the greater fraction of the Ni_4Ti_3 phase.

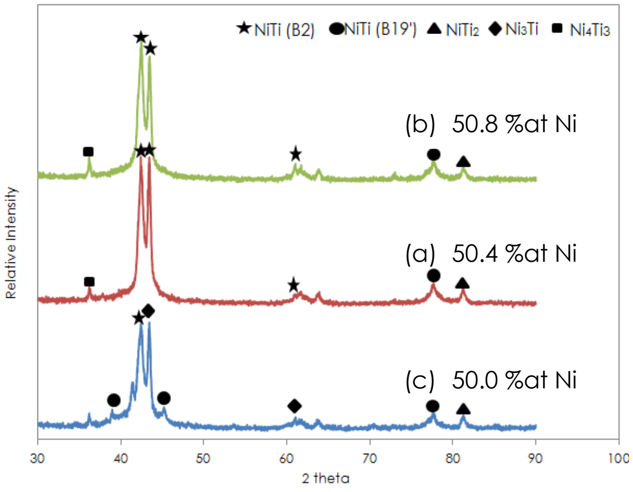

Figure 5 XRD result of the as-sintered sample at 1100˚C

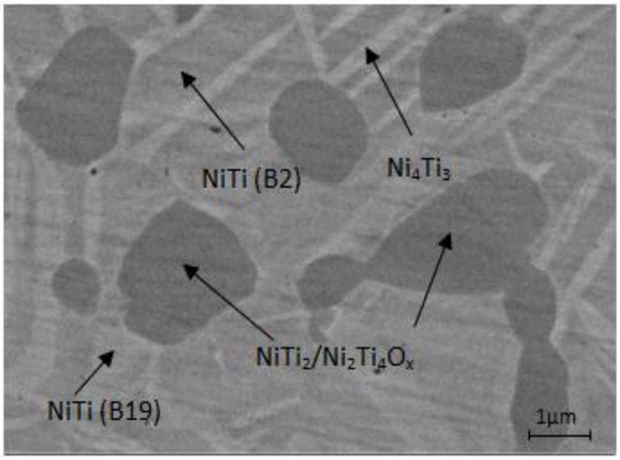

Figure 6 Back scattered SEM of the as-polished 50.4at%Ni alloy

3.3 Phase Transformation Temperatures (PTTs)

Fig. 7 shows the reversible phase transformation temperatures (PTTs) of the as-sintered samples, indicating in each case the approximate reversible martensite (B19') to austenite (B2) PTTs during (a) heating and (b) cooling, respectively. It is apparent that all samples exhibit a reversible transformation during heating and cooling, despite without post heat treatment, which manifest that the significant diffusion between Ni and Ti powders during sintering that led to the formation of transient liquid phase. However, it is expected that some improvements could be achieved with further post treatment such as full annealing and aging processes [8-9].

The figure shows a distinguished transformation peaks between the three samples in which the sample with lowest Ni content (50.0at%Ni) shows a clear single peak (P1) of the reversible austenite to martensite phases transformation. For the Ni-rich compositions (50.4 and 50.8at%Ni), multiple peaks (P1, P2 & P3) could be observed clearly, indicating two-step transformation, the transition between the B2→R-phase→B19'. Su and Wu [13] has reported that the first peak during heating corresponded to two phase transformation from the martensitic phase (B19'→R→B2) and the second peak corresponded to direct transformation from B19' to B2.

In the present work, it obviously shows that the first peaks (P1) for the 50.0at%Ni alloy is approximately 50°C during heating correspond to a complete transformation from the martensite (B19') to austenite (B2) phase. When Ni content is increased, the transformation peak is found to be reduced and widen owing to transition of R-phase during B19'→ B2 transformation. For the 50.4at%Ni the peaks P1, P2 and P3 are approximately 10, 70 and 140°C, respectively, during heating, while for the highest Ni contents (50.8at%Ni) the peaks P1, P2 and P3 are approximately 10, 75 and 150°C, respectively during heating. The austenite finish (A_f) for all samples is around 100°C and above, which is 50°C greater than the previous research conducted by Ismail [12]. This could be attributed from the binder system, whereas in the previous work, the PEG/PMMA binder system was employed. Moreover, the fluctuation of the PTT's could also be either caused by small deviation of Ni and Ti ratio of the tested samples or by the irregularity of the pores structure produced after sintering. The presence of the metastable R-phase is commonly described in a PTT curve, whereas a multistage transformation commonly appears either during heating or cooling and as a consequence, a direct reversible transformation from the austenitic phase to martensitic phase would be more difficult. A higher energy is needed to enable the austenite phase to transform to martensite. However, due to less energy consumed for Ni_4Ti_3 precipitation, the R-phase formation is much more favoured.

Fig. 7(b) shows the DSC curves of the NiTi alloys upon cooling; a broader phase transformation from B2 to B19' could be found with indication of R-phase superposition. The result shows that increasing Ni content results in increasing numbers of transformation peaks; 50.0at%Ni (P1'), 50.4at%Ni (P1' and P2') and 50.8at%Ni (P1', P2' and P3'). The lowest Ni content shows a single complete transformation from martensite to austenite with P1' of ~25°C. For the 50.4at%Ni, the first peak (P1') corresponds to B2→R occurs at ~ 0°C , followed by the second peak (P2') at ~25°C corresponds to R→B19'. The highest Ni contents clearly show three peaks with P1', P2' and P3' of ~ 60, 0 and -25°C, respectively. It is well known that for Ni-rich NiTi alloy, a small increase in the Ni content of 0.1at.% will result in decreasing of the martensite start of about 15K [14]. Besides that, it was also reported that the formation of Ti-rich precipitations such as TiC and $Ni_2Ti_4O_x$ lead to enrichment of Ni in NiTi matrix and consequently responsible for broadening and lowering the PTT [15]. It clearly shows that the PTTs for all samples are within the human body temperature, where mechanical tensile test were performed. Therefore, it is expected that the samples are nearly fully austenitic phase during compression and possibly transform to martensite as the stress is induced.

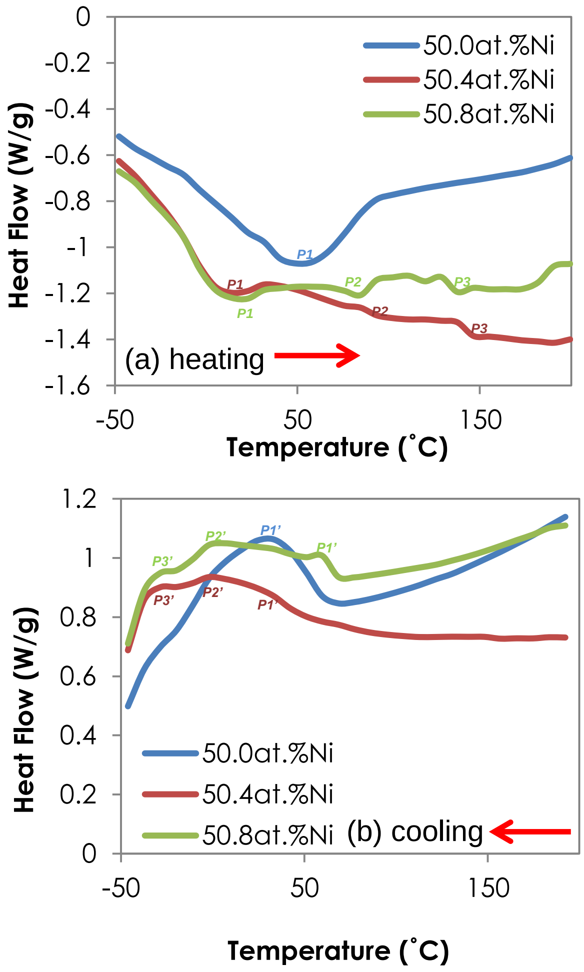

Figure 7 Reversible martensite to austenite transformation during (a) heating and (b) cooling

3.4 Mechanical Behaviour

One of the unique properties of NiTi alloy is low in stiffness, which generally known as Young's modulus, ranging from approximately 28 to 85 GPa, depending on the phases exist; martensitic or austenitic [5]. For many conventional implant metallic materials such as stainless steel 316L-grade and Ti6Al4V alloy, the Young's modulus are 210 GPa and 110 GPa, respectively, which are relatively higher than that of the maximum stiffness of natural bone (20 GPa). The reasons for the current trend in the production of the porous metallic biomaterials implants are (1) open porosity enhances bone ingrowth and thus improve fixation on the interface between bone and implant and (2) porosity decreases the mismatch in stiffness between bone and implant, thus reducing the stress-shielding effects, which shorten the lifetime of the implant through bone resorption [12, 15].

Fig. 8 shows the result of tensile stress-strain curves for the as-sintered NiTi alloys with different Ni-Ti ratios conducted at room temperature (~27°C). It clearly shows that with increased Ni contents the level of ductility is slightly improved, indicating from the maximum final strain before samples completely fractured. The PE behavior is also expected to be improved owing to a major fraction of the austenitic phase as depicted in the XRD results. The Young's modulus calculated from the stress-strain curves for all samples were in the range of 2.5 – 4.0 GPa, which is close to the cancellous type bone (1-2 GPa). Thus, the samples produced could be a possible candidate for bone implant application.

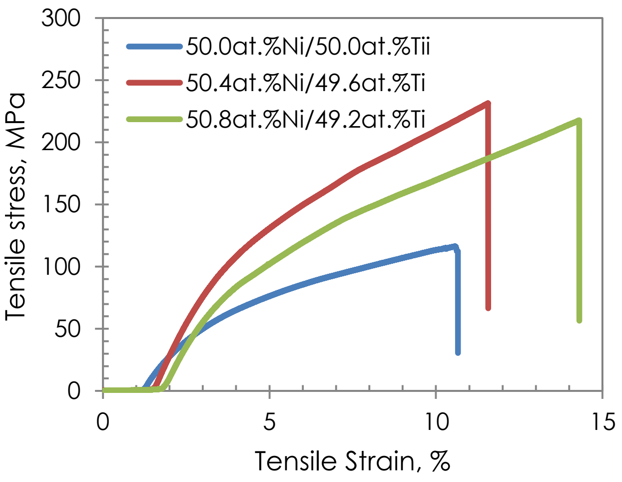

Figure 8 Tensile test behaviour of the as-sintered NiTi alloys

It was noticed that the parts exhibited three distinctive features during tensile:

(1) Linear elasticity: stress and strain are proportional to each other through Hooke's law. A linear relationship was found between stress and the corresponding strain for all conditions, at around 25-100 MPa and 2%, respectively. The slope of this linear region segment corresponds to the stiffness, better known as Young's modulus, E. Owing to a greater fraction of austenitic phase for the Ni-rich alloys (50.4 and 50.8at%Ni), the samples exhibited slightly higher stiffness.

(2) Yielding and plastic deformation. The samples started to yield at a stress of approximately 25 -100 MPa with an associated strain of ≈ 2%, increased slightly with increased Ni content. After yielding, the parts exhibited nearly linear plastic deformation with a long horizontal plateau in the stress-strain curve indicating that the parts were strained hugely with a small increment of stress. For NiTi alloy, this yielding point is generally termed as critical stress owing to the transformation of martensitic phase, which is known to exhibit a lower stiffness than the austenitic phase. The greater the strain plateau region, the more martensitic phase was induced. However, this condition was also attributed by the fraction of secondary phases such as $NiTi_2$ and Ni_3Ti. 3) Plastic collapse. As soon as the tensile stress attained its maximum value, the parts no longer withstood higher loads; the parts started to fracture until completely separated in two pieces. The failure could also be contributed from the porous section in the samples.

Fig. 9 shows the morphology of the fracture samples of (a) 50.0at%Ni and (b) 50.8at%Ni after the tensile test. A unique structure was observed, as previously investigated by Ismail [12], however, the pore structure observed in the present work was much smaller than that of the previous work. This could be due the powder size and the binder system employed; the powder used in the present work was almost half the previous one [12]. The morphology of the fracture sample with the lowest Ni content as shown in Fig 9(a) exhibited larger pore channels in comparison with the highest Ni content (Fig. 9(b)) which contributed to lower mechanical strength as discussed previously. The image clearly shows that the pores are connected to each other by pore channels. The pore structure is irregular, with the pore size being similar to or slightly larger than the particle size in the original mix of elemental powders. The formation of a greater fraction of inter-connected pores after sintering was believed to have originated from the preceding steps prior to sintering, i.e. solvent extraction and thermal debinding, which leave the samples with a greater amount of porosity (a first approximation of the amount of binder used). The pore channels were further enlarged as the sintering progressed, leading to the overall sample expansion, although some samples distorted slightly.

The formation of the liquid phase was believed to be responsible for producing smooth and clean pore channel surfaces, interconnected between the pores. There is no evidence of un-reacted powders in the structure, indicating that the powders were possibly reactively sintered to form NiTi alloy. Several thermal events might have occurred, namely solid-state diffusion, Kirkendall porosity and the transient liquid phase [16]. When observing the fracture surface of pore struts walls, it is clear that most of the surfaces contain many dimples, which indicate ductile behaviour. It is well known for porous NiTi alloys that, particularly Ni-rich alloys, due to excellent PE behaviour, a ductile behaviour has always been reported in literature [17-18]. Nevertheless, in many cases of porous NiTi alloys, because of the existence of the secondary phases in the pore struts walls, which are known to be more brittle than the matrix, the fracture surfaces mainly consist of a combination of ductile and brittle fractures [19]. In the latter type of fracture, cleavage fracture was observed.

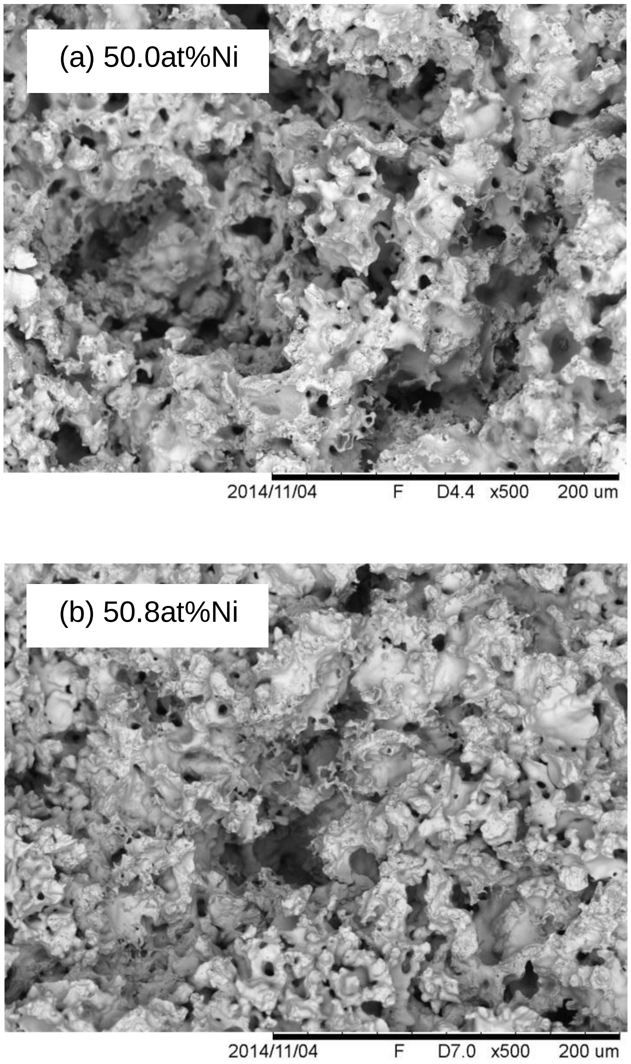

Figure 9 Fracture surface of the samples after tensile test with different Ni content (a) 50.0at%Ni and (b) 50.8at%Ni.

4.0 CONCLUSION

NiTi alloys with different Ni – Ti ratios were successfully produced from the elemental powder of Nickel and Titanium by metal injection moulding. In addition, some conclusions based on the present work can also be drawn as follows:

The feedstock prepared exhibited pseudoplastic behavior at all temperatures tested (110 -150°C); the required flow properties in injection moulding process. Results showed that increasing the Ni content in the formulation resulted in slightly decrease in viscosity, particularly at the lower shear rate which was attributed from the finer powder size of Ni powder. The tensile test samples were successfully injection moulded at barrel temperature of 130°C without any defects.

Fom the XRD results, greater fraction of B2 phase (austenite) was observed for higher Ni contents (50.4at.%Ni and 50.8at.%Ni) in comparison with the 50.0at.%Ni. The back-scattered SEM result clearly showed different gray-scales contrast, indicating different phases exist as a result of different energy absorbed.

The DSC results clearly showed a distinguished transformation peaks between the three samples in which the sample with lowest Ni content (50.0at%Ni) shows a clear single peak (P1) of the reversible austenite to martensite phases transformation. For the Ni-rich compositions (50.4 and 50.8at%Ni), multiple peaks (P1, P2 & P3) could be observed clearly, indicating two-step transformation, the transition between the B2→R-phase→19'. A similar behavior of reverse transformation was also observed during cooling.

The samples exhibited a promising mechanical tensile properties with the Young's modulus calculated from the stress-strain curve in the range of 2.5 to 4.0 GPa which is close to cancellous type bone. The porous structure shown in SEM images was highly inter-connected, thus promoting better bone tissue ingrowth when it is used as an implant. Increaseing Ni contents resulted in slightly increase in degree of ductility which attributed from less fraction of porosity in the samples.

Acknowledgement

The authors would like to thank the Ministry of Education (MOE) and Universiti Teknologi MARA for awarding research grant, RMI/FRGS 5/3 (38/2012) and 600-RMI/RACE 16/6/2 (5/2012) for the financial support to conduct this research.

References

[1] Fuentes, J. S. J. M. G. and Gümpel, P. 2002. Phase Change Behavior of Nitinol Shape Memory Alloys Influence of Heat and Thermomechanical Treatments. *Advanced Engineering Materials*. 7: 437–451.
[2] Fatiha, B., Feninat, E., Laroche, G., Fiset, M. and Mantovani, D. 2002. Shape Memory Materials for Biomedical Applications. *Advanced Engineering Materials*. 3: 91–104.
[3] Schöller, E., Krone, L. Bram, M., Buchkremer, H. P. and Ståaver, D. 2005. Metal Injection Molding Of Shape Memory Alloys Using Prealloyed Niti Powders. *Journal of Materials Science*. 40: 4231–4238.
[4] Bhaumik, S. K. 2011. Nickel-Titanium Base Shape Memory Alloys (SMAs): Smart Metallic Materials," in 6th Symposium on National Frontiers of Engineering.
[5] Thompson, S. A. 2000. An Overview Of Nickel-Titanium Alloys Used In Dentistry. *International Endodontic Journal*. 33(4): 297 - 310.
[6] Machado, L. G. and Savi, M. A. 2003. Medical Applications Of Shape Memory Alloy. *Brazilian Journal of Medical and Biological Research*. 36: 683-691.
[7] Pelton, A., Russell, S. and DiCello, J. 2003. The Physical Metallurgy Of Nitinol For Medical Applications. *Journal of the Minerals, Metals and Materials Society*. 55(5): 33-37.
[8] Elahinia, M. H., Hashemi, M., Tabesh, M. and Bhaduri, S. B. 2012. Manufacturing And Processing Of Niti Implants: A Review. *Progress in Materials Science*. 57(5): 911–946.
[9] Yen, F.-C., Hwang, K.-S., Wu, S.-K. and Wu, S.-H. 2011.TiNi Shape Memory Alloys with High Sintered Densities and Well-

Defined Martensitic Transformation Behavior. *Metallurgical and Materials Transaction A*. 42 (8): 2431–2441.

[10] Razali, R., Abdullah, Z., Subuki, I., Ismail, M. H. and Muhamad, N. 2014. Feedstock Characterization of Elemental Nickel and Titanium Powders Mixture for Metal Injection Moulding Process. *Applied Mechanics and Materials*. 575: 78 - 82.

[11] Azuddin, M., Choudhury, I. A. and Taha, Z. 2012. Development And Performance Evaluation Of A Low-Cost Custom-Made Vertical Injection Molding Machine. *J. Braz. Soc. Mech. Sci. Eng*.1-8.

[12] Ismail, M. H. 2012. Porous Niti Alloy By Metal Injection Moulding (MIM) Using Partly Water Soluble Binder System. University of Sheffield, *PhD Dissertation*.

[13] Su P. C. and Wu S. K. 2004. The Four-Step Multiple Stage Transformation In Deformed And Annealed $Ti_{49}Ni_{51}$ Shape Memory Alloy. *Acta Materialia*. 52: 1117.

[14] Shugo Y., Hanada S. and Honma T.1985. Bull. Res. Inst. Min. Dress. *Metall*. 41: 35.

[15] Ismail, M. H., Goodall, R. Davies, H. A. and Todd, I. 2012. Formation Of Microporous Niti By Transient Liquid Phase Sintering Of Elemental Powders. *Materials Science and Engineering C*. 32(6): 1480–1485.

[16] Whitney, W. Corbin, S. F. and Gorbet, R. B. 2009. Investigation Of The Influence Of Ni Powder Size On Microstructural Evolution And The Thermal Explosion Combustion Synthesis Of Niti. *Intermetallics*. 17(11): 894–906

[17] Köhl M., Habijan T., Bram M, Buchkremer H. P., Stöver D. and Köller M. 2009. Powder Metallurgical Near-Net-Shape Fabrication of Porous NiTi Shape Memory Alloys for Use as Long-Term Implants by the Combination of the Metal Injection Molding Process with the Space-Holder Technique. 11: 959.

[18] Yuan, B., Chung, C. Y. and Zhu, M. 2004. Microstructure And Martensitic Transformation Behavior Of Porous Niti Shape Memory Alloy Prepared By Hot Isostatic Pressing Processing. *Materials Science and Engineering A*. 382(1–2): 181–187.

[19] Lagoudas, Dimitris C., Vandygriff and Eric L. 2002. Processing and Characterization of NiTi Porous SMA by Elevated Pressure Sintering. *Journal of Intelligent Materials Systems and Structures*. 13: 837-850.